Estimating the Critical Density of Road Transportation Networks using Infinitesimal Perturbation Analysis of Hybrid Systems

C. Menelaou, S. Timotheou, P. Kolios, and C.G. Panayiotou

***Abstract*— Traffic congestion can be eliminated by restraining the number of vehicles within an urban region to be below its critical density. To achieve that, [1], [2] proposed a route-reservation architecture that makes appropriate routing schedules according to a region's critical density, and controls vehicle departure times, so that vehicles arrive at their destination in the earliest possible time while avoiding road-segments that are expected to be at their critical density. However, the critical density is not always known and may vary depending on the road conditions.**

In this paper, we adobe the Stochastic Fluid Modeling framework to model the critical density of a homogeneous region of the road network and employ the route-reservation scheme to control traffic within this region for congestion-free operation. To derive the critical density, we employ Infinitesimal Perturbation Analysis (IPA) that provides a stochastic approximation which can be employed in an on-line fashion to capture the dynamic changes in the critical density value as a consequence of different incidents.

I. Introduction

Operating and managing large-scale transportation networks is a challenging task that becomes even harder to tackle as increased demand for mobility results to higher levels of traffic congestion. Traffic congestion is the source of a variety of problems including multiple socio-economic effects ranging for environmental pollution, delays and productivity loss. Congestion occurs as the vehicle density surpasses the network's available capacity [3] while effective management schemes are not in place to prevent network overload in the first place.

Recent advances in Information and Communication Technologies (ICT) enable traffic control mechanisms that can alleviate the traffic congestion problem. One such mechanism has been proposed earlier by the authors in [1], [2] where, in the context of connected-autonomous vehicles, a novel route-reservation architecture (RRA) computes and manages the vehicle routing and schedules them from their origin O to the destination D through non-congested road segments. Guided by the macroscopic traffic theory [4] and assuming that the critical density of each road segment has constant and known value, the key objective of the proposed RRA is to maintain each road's density below the critical value [5]. To to that, the system keeps a record of all reservations made over time and new vehicles are scheduled only via non-congested routes assuming they will travel at the free-flow speed. Therefore, for each vehicle there is a detailed reservation plan with timings along the exact route that it should follow from O to D. An important assumption of the RRA solution is that each segment's critical density is known apriori. However in realistic scenarios the critical density can change over time for a variety of reasons including changes in demand and O-D pairs, changes in flow conditions due to road works or accidents and due to environmental factors such as changing weather conditions.

In this work, we relax the aforementioned assumption on the requirement of knowing apriori the critical density of a particular region of the road network. The aim is to estimate that value in an on-line fashion by employing stochastic fluid modeling (SFM). Inspired by early works done by [6], [7], [8] a region of the road network is modeled as a hybrid system using the SFM framework and Infinitesimal Perturbation Analysis (IPA) is employed in order to compute the gradient of a performance metric which in turn can be used to optimize the selected control parameter. SFM modeling enables the abstraction of a system to a fluid queue and derives gradient estimators for the performance measures of interest (e.g., queue throughput and packet delay) with respect to an assigned control parameter (e.g., buffer maximum content). In addition to optimization, the IPA framework is also utilized for performance-regulation purposes as introduced in [9]. In this work, a single region of the road network is abstracted as a single queue and the gradient estimator obtained through IPA is employed to **estimate** the buffer threshold associated with the critical density of the region. This value can then be employed by the RRA algorithms to compute congestion-free routes over O-D pairs in the specific region of the road network.

Work in transportation networks employing the SFM framework and IPA analysis including [10], [11] try to

This work has been supported by the European Union's Horizon 2020 research and innovation programme under grant agreement No 739551 (KIOS CoE), the Government of the Republic of Cyprus through the Directorate General for European Programmes, Coordination and Development and the European Research Council Advanced Grant FAULT–ADAPTIVE.

C. Menelaou, S. Timotheou, P. Kolios and C.G. Panayiotou are with the KIOS Research and Innovation Center of Excellence, and the Department of Electrical and Computer Engineering, University of Cyprus, {cmenel02, timotheou.stelios, pkolios and christosp }@ucy.ac.cy

solve the traffic-light control problem for a single intersection. A recent work presented in [12] extended the aforementioned approaches to multiple intersections. In these works, the on-line gradient estimators are used to iteratively adjust the optimum light cycle lengths over an average traffic congestion metric with respect to the controllable variables that in turn define the green and red cycle phases. The work in [13] tries to control the red/green phases over a signalizing intersection thus to regulate congestion under a given reference level (queue length). The major advantage of these approaches is that vehicles flow rates are measured on-line only when specific events occur with the gradient estimators obtained only by counting the traffic light switchings.

In this work, IPA analysis is used to estimate the critical density of a region of a road network and enable the route reservation algorithm to prevent congestion without restricting the maximum outflow of the network. According to this setup the main contribution of this paper are:

- The derivation of IPA sensitivity estimates of the performance measure of instantaneous throughput of the whole region with respect to the critical density.
- The on-line application of the derived IPA estimators to the actual system (not the SFM) in order to optimize the critical density selection that is going to be used by the route reservation architecture.
- The proposed model explicitly addresses the two-state traffic dynamics using IPA analysis. According to traffic theory the outflow of a homogeneous region is highly correlated with its instantaneous density as its state can be described in one of two possible regimes: i) the free flow regime and the congested regime. In this work we illustrate how, using IPA analysis, these switching dynamics are taken into consideration to determine the state evolution.

The remainder of this paper is organized as follows: Section II presents the system model and the basic flow control problem for the SFM setting of the route-reservation architecture while the performance metrics of the related problem are also mathematically formulated. Section III derives the IPA estimators for the region's throughput gradients based on the SFM setting. Section IV includes simulation results demonstrating how the SFM-based gradient estimators can be used for the on-line estimation of the critical capacity, showing an approximation method which can be on-line applied to the actual system (not the SFM). Finally, Section V concludes this work and discusses future research directions motivated by this work.

II. System Model and Problem Statement

A. Traffic Flow Model

Consider a *homogeneous* urban road region [14] defined as a graph $\mathcal{G} = (\mathcal{V}, \mathcal{E})$ with vertices $\mathcal{V}$, $N_V = |\mathcal{V}|$,

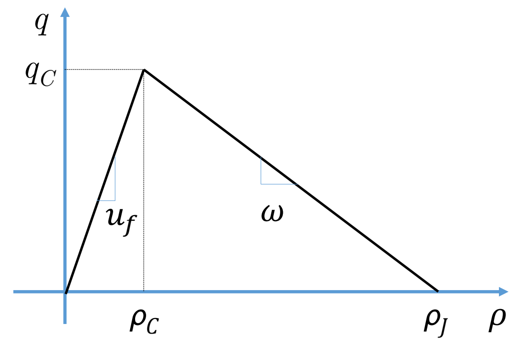

Fig. 1: A triangular Network Fundamental Diagram (NFD) of an urban area.

representing the road-junctions and edges $\mathcal{E}$, $N_E = |\mathcal{E}|$. Due to the homogeneity of the region, the *Network Fundamental Diagram* (NFD) [5] can describe the macroscopic traffic behaviour using three fundamental parameters: *speed*, $u(t)$ (km/h), *flow* $q(t)$ (veh/h), and *density* $\rho(t)$ (veh/km). Fig. 1 depicts a typical flow-density relationship which is comprised of two distinct regimes separated from the *critical density*, ρ_C: 1) the *free-flow regime* where traffic flows at free-flow speed u_f, and 2) the *congested regime* where traffic experiences a speed reduction due to congestion. The flow-density diagram is complemented by the fundamental relationship that the flow is equal to the product of density and speed, i.e., $q(t) = \rho(t)u(t)$. Using this information, one can define other important parameters of the NFD depicted in Fig. 1 such as the *capacity* $q_C = \rho_C u_f$ which is the maximum possible flow of the region observed at the critical density, the *jam density*, ρ_J, and the *backward congestion propagation speed* $w = q_C/(\rho_J - \rho_C)$ [5]. Notice that above the critical density ρ_C the outflow of the region decreases [15].

To maximize the flow through the region, current literature controls traffic to regulate the density of the network below or equal to ρ_C, assuming that the parameters of the NFD are known. Such control mechanisms include perimeter control that regulates exogenous traffic entering the network [16], [17] and route reservations that manage demand from exogenous and endogenous traffic [1], [2].

In this work we consider the use of route-reservations to maintain the traffic density of the region below ρ_C. Route-reservations are used to keep track of the cumulative number of arrivals and departures within the region. Let variable $r(t)$ denote the accumulated number of vehicle reservations within the region, and L the total length of all roads in the region. Then, the quantity $r(t)/L$ approximates $\rho(t)$ at time t. Considering the NFD of Fig. 1 and the fact that the route-reservation scheme operates within the free-flow regime, it is true that vehicles traverse the entire region with a constant speed equal to u_f. Hence, vehicle l entering the region at time t remains within the region up to time $t + t_l$

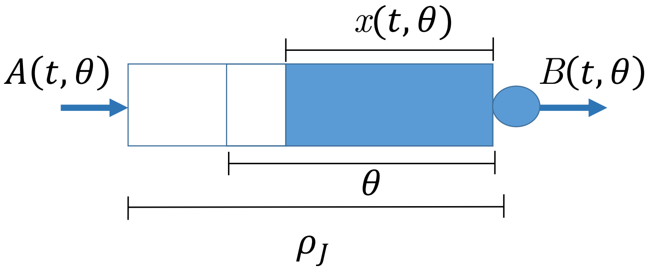

Fig. 2: The corresponding Stochastic Fluid Model (SFM) of the considered network.

where $t_l = L_l/u_f$ denotes the travel time and L_l the route length of vehicle l. Hence, the region is denoted as *admissible* if a vehicle l entering at time t can traverse the region without making the accumulated reserved density larger than the critical density for the entire traversing period. Hence, the *admissibility state* $n(t)$ can be defined as:

$$n(t) = \begin{cases} 1, \text{ if } r(t+k)/L \leq \rho_C, \ \forall\, k \in [0,\ t_l] \\ 0, \text{ otherwise} \end{cases} \tag{1}$$

Therefore, under the route-reservation scheme vehicles are allowed to reserve routes only during time periods where $n(t) = 1$ to ensure that the region never enters the congested regime.

Contrary to previous literature assuming known NFD parameters, this work aims to estimate the critical density by maximizing the outflow of the region. Next, it is described how a Stochastic Fluid Model can be used to represent the traffic network and formulate the investigated problem.

B. Stochastic Fluid Model Representation

The traffic flow model under consideration can be represented as a Stochastic Fluid Model (SFM) based on continuous fluid-flow dynamics characterized by a set of stochastic processes defined on a common probability space $(\Omega, \mathcal{F}, \mathcal{P})$ [18], [19].

As shown in Fig. 2, the road network can be represented by a fluid-storage queue with finite density (content) ρ_J with a single-server to determine the traversal time (service time) of vehicles within the region. The control parameter of interest is θ which denotes the maximum queue size allowed within the queue. Parameter θ is regulated using some control mechanism (in our case route reservations). Parameter θ aims to estimate the critical density in order to maximize the outflow of the queue. According to the NFD, for $\theta > \rho_C$ the region is over-utilized resulting in a reduction of the outflow as the region experiences congestion. On the contrary, for values of $\theta < \rho_C$ the region is underutilized, also resulting in a reduction of outflow. Hence, the aim is to define a strategy that changes online the value of θ in order to operate as close as possible to the critical density of the system that maximizes the outflow.

Let $x(t,\theta)$, $A(t,\theta)$ and $B(t, x(t,\theta))$ denote the SFM state (queue content), arrival rate[1] (inflow) and departure rate (outflow) at time t, respectively.

The arrival rate of vehicles depends on θ and is given by

$$A(t,\theta) = \begin{cases} a(t), & \text{if } r(t) < \theta \\ 0, & \text{if } r(t) \geq \theta \end{cases} \tag{2}$$

where, the variable $a(t)$ denotes the vehicle arrival process which is a time-varying and unknown function independent of θ. According to (2), when the number of reservations reaches the parameter θ (which should approximate the critical density of the region) the inflow is set to zero so that no more vehicles to enter, until $r(t) < \theta$. Here, it is assumed that the reservations are consistent with the actual state of the region ($x(t,\theta) = r(t)$). Although, this is not generally true due to the stochastic nature of traffic [1], [2], it is a reasonable assumption in light of the emergence of connected and automated vehicles.

The departure rate $B(t, x(t,\theta))$ depends on the NFD; when the density exceeds ρ_C the function $B(t, x(t,\theta))$ changes from a linear increasing function (free-flow regime) to a linear decreasing function (congested regime). Hence, $B(t, x(t,\theta))$ is defined as

$$B(t, x(t,\theta)) = \begin{cases} u_f x(t,\theta), & \text{if } \ x(t,\theta) < \rho_C \\ w(\rho_J - x(t,\theta)), & \text{if } x(t,\theta) \geq \rho_C \end{cases} \tag{3}$$

Notice from Eq. (3) that the departure rate is significantly affected by the instantaneous density in two ways: (a) when parameter θ overestimates ρ_C, undesirable vehicle delays are produced that further exacerbate congestion conditions, and (b) when θ underestimates ρ_C the region is underutilized leading to lower outflow rates.

The queue content is determined by the following differential equation:

$$\dot{x}(t,\theta) = \begin{cases} 0, \text{ if } x(t,\theta) = 0 \,\&\, A(t,\theta) = 0, \\ 0, \text{ if } x(t,\theta) = \theta, \\ A(t,\theta) - B(t, x(t,\theta)), \text{ otherwise}, \end{cases} \tag{4}$$

with the initial condition that $x(0) = x_0$, with x_0 known. Here, it is assumed for simplicity that $x(0) = 0$. Note that according to Eq. (4) whenever $x(t,\theta) > 0$ a non-zero flow rate should be observed. Moreover, for the case $x(t,\theta) = \theta$, it may be true that $A(t,\theta) = B(t, x(t,\theta)) \neq 0$ such that $\dot{x}(t,\theta) = 0$. In addition, we make the technical assumption that $a(t) \geq -\epsilon$ where ϵ is a small positive number. This assumption is needed to make sure that the queue becomes empty at a finite time (and does not go to zero asymptotically). For practical systems, this assumption does not have any impact, since $a(t) \geq 0$ and empty periods are always observed.

[1] Consistent with the proposed architecture a central entity is responsible to schedule vehicles according to the described route-reservation scheme. In this way, the arrival rate is controlled to ensure that $x(t,\theta) \leq \theta$.

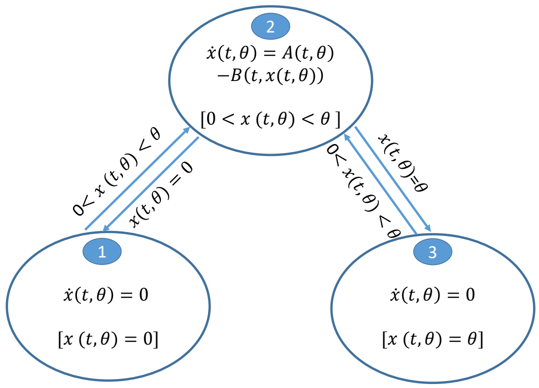

Fig. 3: The Stochastic Hybrid Automaton model.

The above SFM setting can be viewed as a hybrid system, with the time-driven dynamics described by Eq. (4) and with event-driven dynamics denoted by the region's full and empty periods. Hence, the region's operation can be determined with a Stochastic Hybrid Automaton (SHA) as depicted in Fig. 3 which consists of three (3) modes. This model is similar to the one used in [7] (single buffer case), but different as the inflow and outflow rates depend on the parameter θ. Let the time interval $[0, T]$; the region operation can be determined by the set of events $E = \{e_1, e_2, e_3, e_4\}$ defined as:

$e_1 : x(t, \theta) = \theta$, queue reaches capacity.
$e_2 : x(t, \theta) = 0$, queue becomes empty.
e_3 : the sign of $A(t, \theta) - B(t, x(t, \theta))$ changes from positive to negative and queue content ceases to be full.
e_4 : the sign of $A(t, \theta) - B(t, x(t, \theta))$ changes from negative to positive and the queue content ceases to be empty.

All events whose occurrence time depends on the parameter θ are called *endogenous events*, while all other that are independent of the parameter θ are referred to as *exogenous events.*

C. Problem Statement

As mentioned earlier, we seek to estimate the critical density which by definition, is the density that maximizes the average outflow of the region $W(t, \theta)$ over the interval $[0, T]$, defined as follows:

$$W_T(t, \theta) = \frac{1}{T} \int_0^T B(t, x(t, \theta))dt \tag{5}$$

Thus the critical density will be approximated by the control parameter θ that will maximize the outflow following the solution of the optimization problem:

$$\max_{\theta} J(t, \theta) = E[W_T(t, \theta)] \tag{6}$$

In the next section we employ the IPA method to determine the best value for the control parameter θ^* in an online fashion.

III. Infinitesimal Perturbation Analysis (IPA)

A. IPA Review:

Let $v_k(\theta)$ denote the occurrence times of k-th event, then the time derivative of queue content (i.e., $x(t, \theta)$) and event occurrence times (i.e., $v_k(\theta)$) with respect to θ can be expressed as:

$$x'(t, \theta) = \frac{dx(t, \theta)}{d\theta} \quad v'_k(\theta) = \frac{dv_k(\theta)}{d\theta} \tag{7}$$

Let k denote the k-th interval $[v_k, v_{k+1}) \in T$ within which the dynamics of $x(t, \theta)$ are fixed representing the right-hand-side expression of Eq. (4). If the SHA is in mode 2, then the queue content at time $t \; \forall t \in [v_k, v_{k+1})$ is formulated as:

$$\begin{aligned} x(t, \theta) &= x(v_k, \theta) + \int_{v_k}^{t} \dot{x}(\tau, \theta)\, d\tau \\ &= x(v_k, \theta) + \int_{v_k}^{t} (A(\tau, \theta) - B(\tau, x(t, \theta)))\, d\tau \end{aligned} \tag{8}$$

If the SHA is in modes 1 or 3, then

$$x(t, \theta) = x(v_k, \theta) \quad \forall t \in [v_k, v_{k+1})$$

As above, taking the derivatives with respect to θ and let $t = v_k^+$ the boundary initial condition can be obtained as:

$$x'(v_k^+) = x'(v_k^-) + [\dot{x}(v_k^-, \theta) - \dot{x}(v_k^+, \theta)]v'_k \tag{9}$$

Furthermore, taking the derivatives with respect to t in Eq. (4) for all $t \in [v_k, v_{k+1})$:

$$\frac{\partial}{\partial t} x'(t, \theta) = \frac{\partial \dot{x}(t, \theta)}{\partial x} x'(t, \theta) + \frac{\partial \dot{x}(t, \theta)}{\partial \theta} \tag{10}$$

As mentioned earlier, the derivative with respect to θ of each event occurrence time (i.e., v'_k) depends on the type of event that occurs. Hence, a discrete time transition that is independent from θ is an exogenous event with $v'_k = 0$. Otherwise, if event depends on the control parameter θ, a continuously differentiable function $g_k : \mathcal{R}^n \times \Theta \longrightarrow \mathcal{R}$ exist such that $v_k = \min\{t > v_{k-1} : g_k(x(t, \theta), \theta) = 0\}$ (this function constitutes the guard function [19]). Now, taking the derivatives with respect of θ we obtain

$$v'_k(\theta) = -\Big[\frac{\partial g_k}{\partial x} \dot{x}(v_k^-, \theta)\Big]^{-1} \Big(\frac{\partial g_k}{\partial \theta} + \frac{\partial g_k}{\partial x} x'(v_k^-)\Big) \tag{11}$$

Proof of the above expressions (Eq. (9) - (11)) can be found in [19].

B. IPA:

Our solution approach is based on the aforementioned IPA analysis that is used to estimate the gradient of our performance metric e.g., throughput Eq. (13) which in turn is employed within a stochastic approximation based algorithm in order to converge towards to the maximum throughput. In this manner we are interested

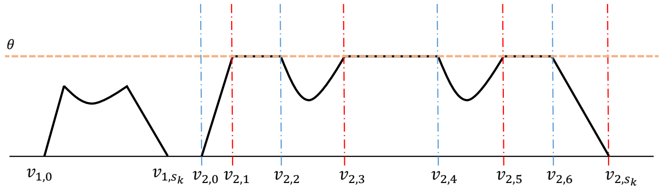

Fig. 4: A typical sample path of the queue's content.

in estimating the $\frac{d}{d\theta}J(t,\theta)$ through an iterative scheme of the form

$$\theta_{k+1} = \theta_k - hH_k(\theta_k, \omega^{SFM}) \tag{12}$$

where h is a constant value step-size and $H_k(\theta_k, \omega^{SFM})$ is an estimate of $\frac{d}{d\theta}J(t,\theta)$ derived on-line and is based on information of its sample path as depicted in Fig. 4.

The related sample path consists of time intervals over which $x(t,\theta) > 0$, called Non-Empty Periods (NEPs), followed by intervals where $x(t,\theta) = 0$, called Empty-Periods (EPs). The k-th NEP period starts at $v_{k,0}$ and ends at v_{k,s_k} where $k = 1, 2, ..., N_T$ and $|N_T|$ denotes the number of NEPs in time-interval T. On that premise some of NEPs may also contain some periods that the system is full at its capacity (FPs) that attain during the interval $[v_{k,2j-1}, v_{k,2j}]$ i.e., $j = 1, \ldots, \frac{s_k-1}{2}$. Note that, the even index $(2j)$ represents the ending time of each particular FP.

Even though the start of a Non-Empty Period looks like an endogenous event (rates $A(t,\theta)$ and $B(t,x(t,\theta))$ generally depend on θ, at the specific time, they are independent of θ. This can be justified combining equations Eq. (3) and (4) as the $x(t,\theta) = 0$ only if $A(t,\theta) = B(t,x(t,\theta)) = 0$ and according Eq. (3) the queue content switches to $x(t,\theta) > 0$ only when the inflow changes from $A(t,\theta) = 0$ to $A(t,\theta) = a(t) > 0$ which is independent of θ. Considering, the SHA in Fig. 3 the transition from mode 2 to 3 is the result of event e_1 which is dependent on θ (endogenous) while the opposite direction (modes 3 to 2) is due to an e_3 event which is independent from θ (exogenous). Considering that during mode 3 $B(t,x(t,\theta))$ is maintained constant and thus the e_3 event occurs only with a decrease of the inflow rate $A(t,\theta) = a(t)$ which is independent from θ. The transition from 2 to 1 (e_2) is considered an endogenous event as its dependent on the queue content. Note that, the times that endogenous events occur indicated with red dashed lines in Figure 4.

Using the above notation, the network's outflow (see Eq. (5)) can be rewritten as:

$$\Omega_T(t,\theta) = \frac{1}{T}\sum_{k=1}^{N_t}\omega_k = \frac{1}{T}\sum_{k=1}^{N_t}\int_{v_{k-1,s_k}}^{v_{k,s_k}} B(t,x(t,\theta))dt \tag{13}$$

where ω_k is the outflow during the kth NEP. Taking derivatives with respect to θ and observing that all EPs are independent from θ then the required IPA gradient derivative $\frac{d}{d\theta}\Omega_T(t,\theta)$ of the Eq. (5)

$$\frac{\partial\Omega_T(t,\theta)}{\partial\theta} = \frac{1}{T}\sum_{k=1}^{N_t}\frac{d\omega_k}{d\theta} \tag{14}$$

The IPA tries to evaluate these derivatives as a function of the observable sample path quantities using similar framework establish in [7], [19]. In this way, the derivation of the IPA derivatives requires some mild assumptions in order to guarantee the existence of derivatives as follows:

1) $A(t,\theta) < \infty$ and $B(t,x(t,\theta)) < \infty$ for all $t \in [0,T]$.
2) For all $\theta \in \Theta$, w.p.1, no two events occur at the same time.

1) Time derivatives: Taking all the possible transition events for a single NEP we have:

At event e_2, a transition from mode 2 to 1 takes place. This is an endogenous event with $g_2(x(t,\theta),\theta) = x(v_{s_k},\theta) = 0$. Applying Eq. (11) we have

$$v'_{s_k} = \frac{-x'(v_{s_k}^-,\theta)}{A(v_{s_k}^-,\theta) - B(v_{s_k}^-,\theta)} \tag{15}$$

In addition applying Eq. (9) we get

$$x'(v_{s_k}^+,\theta) = x'(v_{s_k}^-,\theta) + [\dot{x}(v_{s_k}^-,\theta)]v'_{s_k} \tag{16}$$

and combining the two equations above we have

$$x'(v_{s_k}^+,\theta) = 0 \tag{17}$$

The e_1 event is an endogenous and thus, there exists a continuous differentiable function denoted as $g_1(x(t,\theta),\theta) = x(v_{2j-1},\theta) - \theta = 0 \ \forall \ j = 1,\ldots,\frac{s_k-1}{2}$ and applying Eq. (11) we get

$$v'_{2j-1} = \frac{1 - x'(v_{2j-1}^-,\theta)}{A(v_{2j-1}^-,\theta) - B(v_{2j-1}^-,\theta)} \tag{18}$$

in the sequel combining Eq. (18) with Eq. (9) we have

$$x'(v_{2j-1}^+,\theta) = x'(v_{2j-1}^-,\theta) + [\dot{x}(v_{2j-1}^-,\theta)]v'_{2j-1} \tag{19}$$

and combining the two equations above Eqs. (19)-(18) we get

$$x'(v_{2j-1}^+,\theta) = 1 \tag{20}$$

The e_3 is an exogenous event with $x'(v_{2j},\theta) = 0 \ \forall \ j = 1,\ldots,\frac{s_k-1}{2}$.

Finally from Eqs. (17)-(20) it follows that $x'(t,\theta)$ always starts from 0 and at every FP switches to 1 and always at the end of the NEP reset back again to 0 value.

2) IPA for throughput:

Lemma 1: Eq. (13) measures the total outflow as the summation of region's NEPs starting from the beginning of an EP until the beginning of the next EP. Therefore, considering that the region's outflow rate is determined by Eq. (3) then taking the derivatives with respect to θ we get

$$\frac{d\omega}{d\theta} = \frac{1}{T}\Big[\sum_{j=1}^{\frac{s_k-1}{2}} C(v_{2j-1} - v_{2j})\Big] \quad (21)$$

where the parameter C is obtained from $B(t, x(t, \theta))$ defined by Eq. (3) and thus

$$C = \frac{\partial}{\partial x} B(t, x(t, \theta)) = \begin{cases} u_f, & \text{if } \ x(t, \theta) \leq \theta \\ -w, & \text{otherwise} \end{cases} \quad (22)$$

Proof: Considering that Eq. (13) can be re-stated as

$$\Omega_T(t, \theta) = \frac{1}{T}\sum_{k=1}^{N_t}\Big[\int_{v_{k-1,s_k}}^{v_{k,0}} B(t, x(t, \theta))dt + \int_{v_{k,0}}^{v_{k,s_k}} B(t, x(t, \theta))dt\Big] \quad (23)$$

then, taking the derivative with respect to θ we get

$$\frac{d\omega_k}{d\theta} = \frac{1}{T}\frac{d}{d\theta}\int_{v_{k,0}}^{v_{k,s_k}} B(t, x(t, \theta))dt \quad (24)$$

since, $\frac{d}{d\theta}\int_{v_{k-1,s_k}}^{v_{k,0}} B(t, x(t, \theta))dt$ is zero as $B(t, x(t, \theta)) = 0$ during an EP. In the sequel, considering the Leibniz rule the above derivative can be computed as

$$\frac{d}{d\theta}\int_{v_{k,0}}^{v_{k,s_k}} B(t, x(t, \theta))dt = B(v_{k,s_k})v'_{k,s_k} + \int_{v_{k,0}}^{v_{k,s_k}} \Big[\frac{\partial}{\partial x}B(t, x(t, \theta))\frac{\partial x}{\partial \theta} + \frac{dB(t, x(t, \theta))}{d\theta}\Big]dt \quad (25)$$

considering the Eq. (25) we can observe that the term $\frac{dB(t,x(t,\theta))}{d\theta} = 0$ as is not dependent on θ while the term $\int_{v_{k,0}}^{v_{k,s_k}} \frac{\partial x}{\partial \theta}$ can be computed as follows:

Considering a single NEP, the term $\int_{v_0}^{v_{s_k}} \frac{\partial x}{\partial \theta}dt$ can be expressed as

$$\int_{v_0}^{v_{s_k}} \frac{\partial x}{\partial \theta}dt = \int_{v_0}^{v_1} x'(t, \theta)dt + \sum_{j=1}^{\frac{s_k-1}{2}}\int_{v_{2j-1}}^{v_{2j}} x'(t, \theta)dt + \sum_{j=1}^{\frac{s_k-3}{2}}\int_{v_{2j}}^{v_{2j+1}} x'(t, \theta)dt + \int_{v_{s_k}}^{v_{s_k-1}} x'(t, \theta)dt \quad (26)$$

Taking one term at time then, during the all the FPs the queue content $x(t, \theta) = \theta$ and thus

$$\sum_{j=1}^{\frac{s_k-1}{2}}\int_{v_{2j-1}}^{v_{2j}} x'(t, \theta)dt = \sum_{j=1}^{\frac{s_k-1}{2}}\int_{v_{2j-1}}^{v_{2j}} 1dt \quad (27)$$

According to Eq. (25) and considering the interval in-between two consecutive FPs the buffer content can be calculated as

$$x(t, v_{2j+1}) = x(v_{2j}, \theta) + \int_{v_{2j}}^{v_{2j+1}} \dot{x}(\tau, \theta) \quad (28)$$

for all $j = 1, \ldots, \frac{s_k-3}{2}$. Then, taking the derivatives with respect to θ and considering that $x(t, v_{2j+1}) = x(v_{2j}, \theta) = \theta$ then we get that

$$v'_{2j+1}\dot{x}(v_{2j+1}, \theta) - v'_{2j}\dot{x}(v_{2j}, \theta) + \int_{v_{2j}}^{v_{2j+1}} x'(\tau, \theta) = 0 \quad (29)$$

for all $j = 1, \ldots, \frac{s_k-3}{2}$. However, considering that $\dot{x}(v_{2j+1}) = v'_{2j} = 0$ then we have

$$\sum_{j=1}^{\frac{s_k-3}{2}}\int_{v_{2j}}^{v_{2j+1}} x'(t, \theta)dt = 0 \quad (30)$$

In similar way, during the interval $[v_0, v_1]$ we get

$$\int_{v_0}^{v_1} x'(t, \theta)dt = 1 \quad (31)$$

while during the interval $[v_{s_k-1}, v_{s_k}]$ we have

$$\int_{v_{s_k}}^{v_{s_k-1}} x'(t, \theta)dt = -1 \quad (32)$$

Therefore, according to Eq. (25) the $\int_{v_0}^{v_{s_k}} \frac{\partial x}{\partial \theta}$ has a unit value only during each FPs while it first and last terms are cancel then its follows that

$$\frac{d}{d\theta}\int_{v_{k,0}}^{v_{k,s_k}} B(t, x(t, \theta))dt = + \sum_{j=0}^{\frac{s_k-1}{2}}\int_{v_{2j-1}}^{v_{2j}} \frac{d}{dx}B(t, x(t, \theta))dt \quad (33)$$

then combining Eqs. (24)-(33) then Eq. (21) follows. ■

IV. Simulation Results

The area under consideration is an 1 km^2 homogeneous [14] region with the following NFD parameters: ρ_C =300 veh/km, ρ_J = 1000 veh/km and u_f =15 m/s all defined over the triangular macroscopic fundamental diagram as denoted by eq. (3) [5].

The actual system is simulated along side the route-reservation algorithm as presented in [1] where each vehicle arrives to the simulated region with a Poisson arrival process. The RRA [1] reschedules the vehicle departure times from their origin according to its objective (that is, maintain each road-segment's density below the critical density). Furthermore, the RRA determines each vehicle's route such that congested links are avoided. To achieve this, the RRA assumes that it knows every link's critical capacity and can determine the exact path of each vehicle assuming that it will traverse its path using the free flow speed u_f. In earlier works, the critical density was measured (through extensive simulation) a priori and it was assumed known by the RRA. In this work, the RRA utilizes an estimate of the critical density θ, which is continuously updated such that RRA is able to learn on-line the true value of the critical density.

For the assumed network, Fig. 5 depict the region's outflow as a function of the critical density assumed by

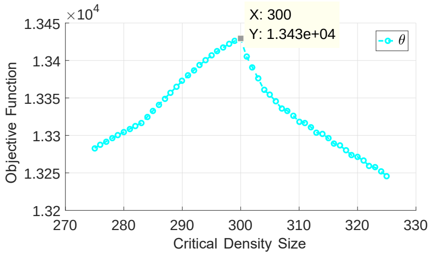

Fig. 5: Region's outflow rate as a function of θ.(Brute-force method)

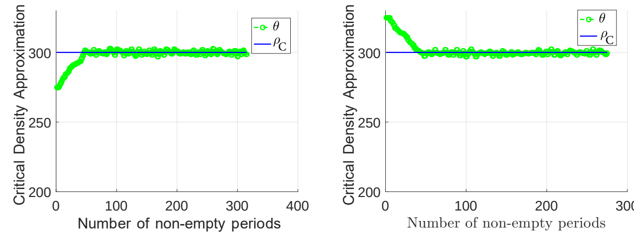

(a) (b)

Fig. 6: IPA estimators starting from different initial values: (a) θ = 275veh/km (b) θ = 300veh/km as a function of the number of NEP observed within the simulation time (iterations).

the RRA. This result is obtained by running long simulations with varying θ within the range of $[275, \ldots, 325]$ in a brute-force manner. As observed by the Fig. 5 the maximum outflow-rate is obtained when $\theta = 300$veh/km while, as expected, for all other values lower flow-rates are observed since using these values imply that the region is under/over utilized.

The critical density estimated by the RRA is updated through the stochastic approximation rule

$$\theta_{i_{k+1}} = \theta_{i_k} - h\frac{\partial \Omega_T(t,\theta)}{\partial \theta} \tag{34}$$

with h denoting the step size while $\frac{\partial \Omega_T(t,\theta)}{\partial \theta}$ denotes the sensitivity of the region's outflow with respect to the parameter θ as computed by the IPA (eq. (21)). At this point it is worth pointing out that despite the fact that the IPA algorithm was derived based on an SFM, the underlying system model used for the simulations is a more realistic discrete event model.

As mentioned above, as the region's density is maintained within the free-flow regime, the outflow has different rate compared to that of the congested regime, fact that can be justified by findings in Fig. 5. Therefore, the derived gradient estimator of Eq. (21) requires the value of the parameter c (see eq. (22)) which is not know since the true state of the network is also not known. In such manner, Eq. (22) approximates all the unknown parameters and the direction of our stochastic approximation algorithm. Notably, considering Eq. (22) the sign of parameter C is highly correlated with the region's state as is depends on whether the estimated parameter θ over/under estimates the actual ρ_C. Since the region's true critical density is not known, it is a challenge to determine the true state of the network.

To address this challenge, we utilize on-line measurements of the outflows of the actual discrete event system. In this way, the parameter C is approximated with the parameter $\hat{C}$, by sampling the region's outflow rate every time that the control parameter θ updates. More specific, we compute the average change of the outflow rate by taking real time measurements across the current and the previous state θ updates (i.e., θ_k and θ_{k-1}) as follows

$$\hat{C} = \frac{\bar{q}(\theta_k) - \bar{q}(\theta_{k-1})}{\Delta L} \tag{35}$$

with the parameter $\bar{q}(\theta)$ denotes the real time measurement of region's outflow as a function of θ and the parameter $\Delta L = |\theta_k - \theta_{k-1}|$ denotes the difference of θ values of the two measurements (this approximation is called as the "Euler's" backward derivative approximation method). In this manner, every time that we are going to update the new θ_{k+1} value we compare the previous measured outflow with the current observation in order to drive the estimated $\hat{C}$. Notably, to further improve the approximation accuracy measurements are taken only during the FPs where the outflow has its maximum possible rate according to the current θ value.

The obtained results of the on-line estimation of $\frac{\partial \Omega_T(t,\theta)}{\partial \theta}$ are depicted in the Fig. 6 which indicate how θ is updated assuming different initial values of θ. In this figure with the green color scatters we denote the updates θ_{k+1} observed on each NEP while with the solid blue line represents the true value of ρ_C =300veh/km. According to the figure, it is clear that for both of these cases the IPA estimates can be used to learn the true critical density irrespective of the initial values. Note that, in the first case of Fig. 6(a) the initial value under-estimated while, in the second case Fig. 6(b) over-estimate the true critical density.

Figs. 7 illustrates scenarios where the actual critical density starts with the initial value of ρ_C =300veh/km while at some point during the simulation time ρ_C suddenly changes due to external factors (e.g., weather conditions) either increases or decreases. In a similar manner with Fig. 6, with the green color scatters we denote the θ_{k+1} as they are updated on every NEP while with the solid blue line we depict the true value of ρ_C. The first two figures Figs. 7 (a) and (b) start with a parameter θ that under-estimates ρ_C and as time progresses it can efficiently approximates the initial critical density value. Subsequently, when ρ_C suddenly changes, it automatically learns that and quickly it converges to the new ρ_C. The same behavior is observed when the critical density value increases or decreases Figs. 7 (a) and (b), respectively.

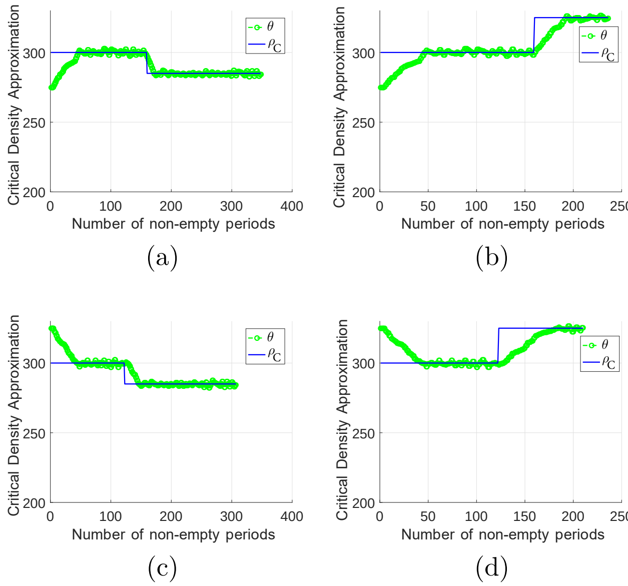

Fig. 7: IPA estimators starting from different initial values with a suddenly change of ρ_C value: (a) and (b) with initial value starting from 275veh/km to 285veh/km and 315veh/km, respectively while (c) and (d) with initial value starting from 325veh/km to 285veh/km and 315veh/km, respectively as a functions of the number of NEP observed within the simulation time (iterations).

V. Conclusions

In this paper we propose a stochastic fluid model with switching dynamics that can be utilized for the online estimation of the critical density of an urban area. The approach, utilizes a stochastic approximation based algorithm that seeks to learn the region's critical density. The stochastic approximation algorithm is driven by sensitivity estimates that are obtained through IPA on stochastic fluid models. The IPA estimate requires minimal information (e.g., timers and average speeds and flow rates). An important challenge of the derived IPA estimator is that it requires knowledge of the state of the network (free flow or congested), which is information not directly observable, however, it is information that can be inferred from the average speed. Thus, the major advantage of this approach in that is mainly the simple implementation and its on-line execution.

Future work includes, the proof of the unbiasedness of the derived estimators which constitute a more difficult task compared to earlier works in IPA on SFM due to unobservable switching dynamics. Future avenues also include the introduction of uncertainty to route-reservation estimates, something that allows the formation of queue that are longer than the region's actual critical density. This will constituted a more realistic approach as in real application inaccuracies maybe observed within the reservation plan [1], [2]. Finally, future work should also examine how the perturbations are propagated between neighboring regions.

References

[1] C. Menelaou, P. Kolios, S. Timotheou, C. Panayiotou, and M. Polycarpou, "Controlling road congestion via a low-complexity route reservation approach," *Transportation Research Part C: Emerging Technologies*, vol. 81, pp. 118–136, 2017.

[2] C. Menelaou, S. Timotheou, P. Kolios, and C. G. Panayiotou, "Improved road usage through congestion-free route reservations," *Journal of the Transportation Research Board*, vol. 2621, pp. 71–80, 2017.

[3] C. Chen, Z. Jia, and P. Varaiya, "Causes and cures of highway congestion," *IEEE Control Systems Magazine*, vol. 21, no. 6, pp. 26–32, 2001.

[4] S. Hoogendoorn and V. Knoop, *Traffic flow theory and modelling*. Edward Elgar Publishing Limited, 12 2012.

[5] L. Immers and S. Logghe, *Traffic flow theory*, Department of Civil engineering Section Traffic and Infrastructure, Belgium, 05 2003, course H 111.

[6] C. G. Panayiotou, "Infinitesimal perturbation analysis for a single stochastic fluid model node with a class of feedback controlled traffic," in *In proceedings of American Control Conference, 2004.*, vol. 3. IEEE, 2004, pp. 2308–2313.

[7] C. G. Cassandras, Y. Wardi, B. Melamed, G. Sun, and C. G. Panayiotou, "Perturbation analysis for online control and optimization of stochastic fluid models," *IEEE Transactions on Automatic Control*, vol. 47, no. 8, pp. 1234–1248, 2002.

[8] H. Yu and C. G. Cassandras, "Perturbation analysis for production control and optimization of manufacturing systems," *Automatica*, vol. 40, no. 6, pp. 945–956, 2004.

[9] Y. Wardi, C. Seatzu, X. Chen, and S. Yalamanchili, "Performance regulation of event-driven dynamical systems using infinitesimal perturbation analysis," *Nonlinear Analysis: Hybrid Systems*, vol. 22, pp. 116–136, 2016.

[10] C. G. Panayiotou, W. C. Howell, and M. Fu, "Online traffic light control through gradient estimation using stochastic fluid models," *In Proceedings of IFAC Volumes*, vol. 38, no. 1, pp. 90–95, 2005.

[11] R. Chen and C. G. Cassandras, "Stochastic flow models with delays and applications to multi-intersection traffic light control," *Systems and Control*, 2017.

[12] Y. Geng and C. G. Cassandras, "Multi-intersection traffic light control with blocking," *Discrete Event Dynamic Systems*, vol. 25, no. 1-2, pp. 7–30, 2015.

[13] Y. Wardi and C. Seatzu, "Infinitesimal perturbation analysis of stochastic hybrid systems: Application to congestion management in traffic-light intersections," in *Proceedings Decision and Control (CDC), 2014 IEEE 53rd Annual Conference.* IEEE, 2014, pp. 6752–6757.

[14] A. Mazloumian, N. Geroliminis, and D. Helbing, "The spatial variability of vehicle densities as determinant of urban network capacity," *Philosophical Transactions of the Royal Society of London A: Mathematical, Physical and Engineering Sciences*, vol. 368, no. 1928, pp. 4627–4647, 2010.

[15] C. F. Daganzo, "Urban gridlock: macroscopic modeling and mitigation approaches," *Transportation Research Part B: Methodological*, vol. 41, no. 1, pp. 49–62, 2007.

[16] M. Keyvan-Ekbatani, A. Kouvelas, I. Papamichail, and M. Papageorgiou, "Exploiting the fundamental diagram of urban networks for feedback-based gating," *Transportation Research Part B: Methodological*, vol. 46, no. 10, pp. 1393–1403, 2012.

[17] J. Haddad and N. Geroliminis, "On the stability of traffic perimeter control in two-region urban cities," *Transportation Research Part B: Methodological*, vol. 46, no. 9, pp. 1159–1176, 2012.

[18] C. G. Cassandras and S. Lafortune, *Introduction to discrete event systems*. Springer Science & Business Media, 2009.

[19] Y. Wardi, R. Adams, and B. Melamed, "A unified approach to infinitesimal perturbation analysis in stochastic flow models: the single-stage case," *IEEE Transactions on Automatic Control*, vol. 55, no. 1, pp. 89–103, 2010.